Spin transport after ultra-fast demagnetization

T. Kieboom

Studentnummer 3946274

Universiteit Utrecht

June 15, 2016

Abstract

In this thesis we discuss spin transport after ultra-fast demagnetization. First we review the microscopic 3 temperature model (M3TM) which describes the local changes of magnetization after exciting a metal with a laser pulse, which heats up the electrons. After this review we study some simple spin currents from ferromagnetic to non-magnetic materials. In particular we solve one stationary solution, and one time-dependent solution. We finish with description of demagnetization which combines the local effects with spins currents (global effects). We find that including the spin transport speeds up the demagnetization effect.

Contents

1 Introduction

In this thesis we are going to discuss spin transport after ultra-fast demagnetization. Ultra-fast demagnetization is a phenomenon discovered in 1996 by Beaurepaire et al.[1]. Beaurepaire experimented with shooting laser pulses on nickle and observed remarkable fast demagnetization. Ultra-fast demagnetization is demagnetization occurring after a laser pulse, with typical time scales from sub-100 fs up to approximately 200 ps, depending on the material. A phenomenological description was readily given by the discoverer himself and is known as the 3 temperature model (3TM). It took however more then 10 years before a good microscopic description was given by B. Koopmans et al. in 2009 by the name microscopic 3TM. [2] The M3TM model is however too simple, and in particular does not account for spin transport phenomena. Therefore the model has to be extended to properly explain more elaborate experiments. In this thesis we present such an extension, based on work by Koopmans.[3]

The thesis is organized as follows: first we discuss the M3TM model, which explains the results found by Beaurepaire. Then we are going to discuss spin transport, which is a crucial part of the extension proposed by Koopmans. After discussing the general framework of spin transport we do some numerical calculations on simple spin transport problems, namely a stationary solution and a simple time dependent solution. We finish with a combination of the M3TM and spin transport, which was proposed by Koopmans.

2 M3TM

In the 3 temperature model we associate a temperature and heat capacity with the spin (T_s, C_s), the electron (T_e, C_e) and the phonon system (T_p, C_p). Heat flows from the systems of high temperature to the systems of low temperature, and the magnitude of the heat current is proportional to the difference of the temperature of two systems. The change of temperature of a system is inversely proportional to the heat capacity of the system. We assume $C_e, C_p \gg C_s$, therefore we can neglect the heat flow to the spin system and assume that $T_e = T_s$. We also assume that the heat flow from the phonon to the spin system is much smaller then from the electron to the spin system. Therefore we neglect the heat flow from the phonon to the spin system. The assumption we make by assigning a temperature to each subsystem is that the internal equilibration of a system is much faster than the heat flows between the systems. Temperature is namely only properly defined in equilibrium.
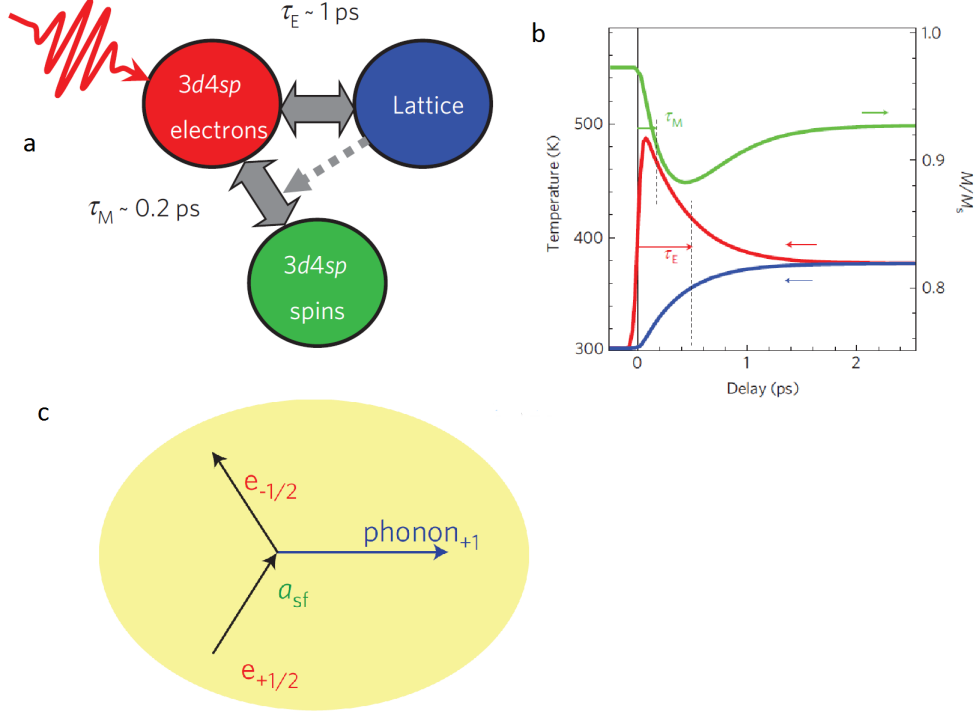
Figure 1: a. The heat exchange between the systems is indicated with double arrows and angular momentum exchange with the dashed arrow. b. The temperature of the electron (red) and phonon (blue) system together with the magnetization (green) as function of time. c. The exchange of angular momentum from electrons to phonons. Picture taken from [2].

The microscopic model consists of a microscopic description of the electron, phonon and spin system and their interactions. The electron system is modeled by non-interacting electrons, the phonon system is described by the Debye model, and the spin system by the Weiss model. The interactions are described by a Hamiltonian which takes into account the electron-phonon scattering without spin flips, and another Hamiltonian which takes into account the electron phonon scattering with spin flips. The scattering probabilities are calculated by using Fermi's Golden Rule for these scattering Hamiltonians. See figure 1a for a schematic depiction of the interactions. Combining these implies

$$C_e[T_e]\frac{dT_e}{dt} = \nabla_z(k\nabla_z T_e) + g_{ep}(T_p - T_e); \tag{1}$$

$$C_p[T_p]\frac{dT_p}{dt} = g_{ep}(T_e - T_p); \tag{2}$$

$$\frac{dm}{dt} = Rm\frac{T_p}{T_C}\left(1 - m\coth\left(\frac{mT_C}{T_e}\right)\right), \tag{3}$$

with

$$R = \frac{8a_{sf}T_C^2 g_{ep}}{k_B T_D^2 D_s}. \tag{4}$$

4

Here, κ is the thermal conductivity, g_{ep} the electron-phonon interaction constant, m the magnetization, a_{sf} the spin-flip probability (the chance a spin flips when a phonon and an electron interact), T_C the Curie temperature, k_B the Boltzmann constant, T_D the temperature associated with the cut-off energy of the Debye model and D_s is the average spin density per atom.[1][2][4]

There are some interesting remarks to make about this set of differential equations. Equation 1 shows the change in time of the electron temperature. This change is slower when C_e is higher, and the change is faster when the difference between T_e and T_p is larger. This corresponds with our usual ideas about temperatures. The temperature of the spin system has a negligible effect on the electron temperature, this is due to $C_e \gg C_s$ while C_p is much closer to C_e. Diffusion is also affecting the change in time of T_e. Which is larger when the spatial variation of T_e is larger. The behaviour of the phonon temperature which is described by equation 2 is similar. There is however no diffusion term, the diffusion of phonons is namely very small compared to the demagnetization processes. Finally, equation 3 can be interpreted as follows: The typical time evolution of this process is depicted in figure 1b. When the laser pulse arrives around $t = 0$, the electrons (red line) start to heat up. When electrons are excited to higher energy levels the spin is conserved due to the optical selection rules, heat will start to flow from the electron system to the lattice and spin systems. Adding energy to a ferromagnetic spin system implies demagnetization, since magnetic interaction favours alignment of spins while thermal fluctuations destroy this alignment. Since $C_e \gg C_s$, T_s changes very fast but barely effects T_e. C_p is however comparable to C_e, therefore the thermalization will proceed much slower. Hence $T_e = T_s$ much earlier then $T_e = T_s = T_p$. When the temperature is equal in all systems, the heat is spread most and the temperature for every system will be lowest. Therefore $T_e = T_s \neq T_p$ is associated with a lower magnetization then $T_e = T_s = T_p$. This is exactly what we observe in figure 1b.[2]

For many phenomena the M3TM is too simple. One of its flaws is the lack of spin transport terms. Take for example the following experiment performed by Malonowski [5]: if one shoots a femto second laser pulse on a magnetic bi-layer one observes a difference in demagnetization of the parallel and anti parallel configuration, see figure 2. This is due to electrons traveling up and down after excitation, which exchanges angular momentum between layers. In the parallel layers this does not cause change in magnetization, but in the anti-parallel layers it does. This induces extra demagnetization which is not taken into account in the M3TM, which is only a local theory. To describe this experiment, and many others, including spin transport is essential. Therefore we need to extend the M3TM.

We will proceed by starting with a phenomenological description of electron and spin transport. This description will be applied to two simple systems, namely a stationary one dimensional system and a one dimensional system with a step function of chemical potential as initial condition. Hereafter we start studying a differential equation proposed by Koopmans, which combines the M3TM with spin transport.

---

[1]For a more elaborate description see chapter 5 of the thesis 'Manipulating Spins' by S. Schellekens [4].
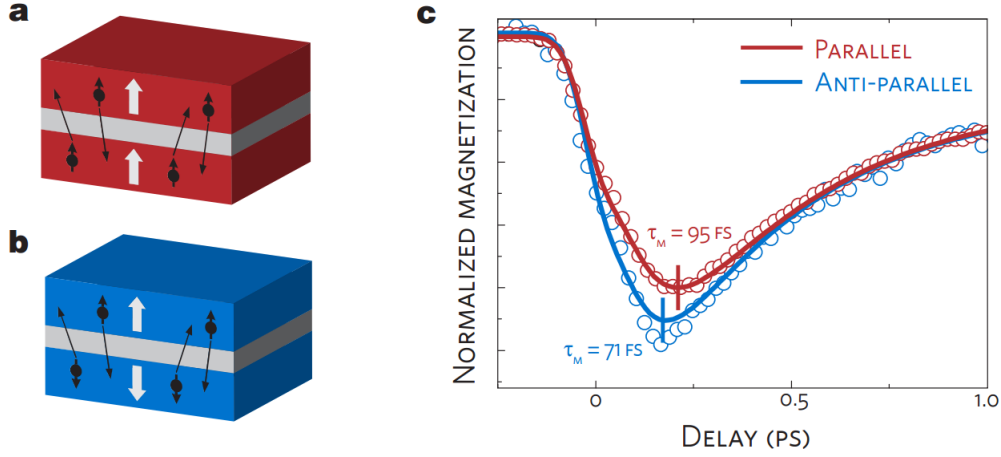
Figure 2: In this experiment a laser pulse is fired on a piece of metal, like the experiment of Beaurepaire. Unlike the experiment of Beaurepaire however, the piece of metal consists of a non magnetic layer sandwiched between magnetic layers. When the Magnetic layers are anti-parallel one observes a stronger demagnetization than the parallel configuration.[5]

3 Spin Transport

First we start with a phenomenological description of the electron currents in ferromagnetic metals (FM) and non magnetic metals (NM). The electrons are the spin carriers, so taking into account the electron movement is essential. The resistance of electrons in FM is namely dependent on the magnetization. [6] The current is therefore by linear approximation given by the following expression:

$$j_\pm = -\sigma_\pm \nabla \mu_\pm / e. \tag{5}$$

With j_+ and j_- the current of the spin up and down electrons respectively, σ_+ and σ_- the conductivity of spin up en down respectively, and μ_+ and μ_- the chemical potential of spin up and down respectively. Since σ_+ and σ_- are constants, we can write $\sigma_+ = \alpha\sigma$ and $\sigma_- = (1-\alpha)\sigma$ with σ the total conductivity and $\alpha \in [0,1]$. Due to the lack of magnetization in NM $\alpha = 0.5$, thus $\sigma_+ = \sigma_-$. For the total current we define $j_e \equiv j_+ + j_-$ and for the spin current $j_s \equiv j_+ - j_-$. For the chemical potential we define $\mu_e \equiv (\mu_+ + \mu_-)/2$ and $\mu_s \equiv \mu_+ - \mu_-$. As a result of conservation of charge the following relation holds:

$$\frac{\partial \rho_e}{\partial t} + \nabla \cdot j_e = 0, \tag{6}$$

with ρ_e the current density. For spin current we have the following continuity relation [6]:

$$\frac{\partial \rho_s}{\partial t} + \nabla \cdot j_s = -\Gamma \mu_s, \tag{7}$$

with ρ_s the spin density and Γ the spin decay rate. Contrary to conservation of charge, the spin density is not conserved. This caused by spin relaxation that are for example mediated by Elliott-Yafet-like processes.[1]

3.1 Stationary solution

To describe an interesting physical system we first model a simple system. After finding a good model for the simple system we elaborate it, such that we finally get a good description of the experiment we are interested in. The system we start with is a piece FM and a piece of NM. The FM reaches from $x = -\infty$ till $x = 0$ and the NM from $x = 0$ till $x = \infty$. We ignore the dependence of the y and z components. We will first solve this system for the time independent case. Hence:

$$\frac{\partial \rho_e}{\partial t} = \frac{\partial \rho_s}{\partial t} = 0. \tag{8}$$

This implies for NM (so $\sigma_+ = \sigma_-$) that

$$\nabla^2 \mu_e = 0 \tag{9}$$

and

$$\nabla^2 \mu_s = \frac{1}{l_s^2} \mu_s, \tag{10}$$

with $l_s = \sqrt{\sigma/\Gamma e}$.

For FM this implies

$$\frac{\sigma_+}{e} \nabla^2 (\mu_s + 2\mu_e) = \Gamma \mu_s \tag{11}$$

and

$$\frac{\sigma_-}{e} \nabla^2 (\mu_s - 2\mu_e) = \Gamma \mu_s. \tag{12}$$

To solve these expressions with respect to x, we first need to impose boundary conditions. The first condition we impose is the existence of a current. We choose $j_e[x] = c$. The choice of x doesn't matter, we arbitrarily pick $x = 0$. The choice of c has to be physically realistic for quantitative predictions, but we are interested in the qualitative behavior. Accordingly we choose again arbitrarily $c = 20 s^{-1} m^{-2}$.

We also state that the current is not discontinuous on the NM/FM interface, so $j_{eNM}[0] = j_{eFM}[0]$. This is equivalent with stating that electrons don't appear or disappear at the boundary. We also assume that the spin current is not discontinuous, so $j_{sNM}[0] = j_{sFM}[0]$. This implies that there is no arbitrarily fast temporary spin flip increase located at the boundary.

We also impose that $\mu_{eNM}[0] = \mu_{eFM}[0]$ and $\mu_{sNM}[0] = \mu_{sFM}[0]$, which means no boundary resistance. We solved the differential equations with the appropriate boundary conditions in Mathematica. For the plots of the solutions see figure 3 and 4.

For the stationary solutions of the electric current, figure 3, we find the currents to be constant. This has to be the case. To understand this, assume there is a varying current distribution. This will cause accumulations of charge which will cause an aggregate electrons to accelerate more in a particular direction, and therefore the current to accelerate. The solution is then not anymore stationary per definition. Since the current is proportional with the gradient of the chemical potential and the conductivity, and the conductivity is a constant for each material (see equation 5). We expect therefore the chemical potential to be a constant slope for $x < 0$ and $x > 0$. This is exactly what we observe in our calculation.
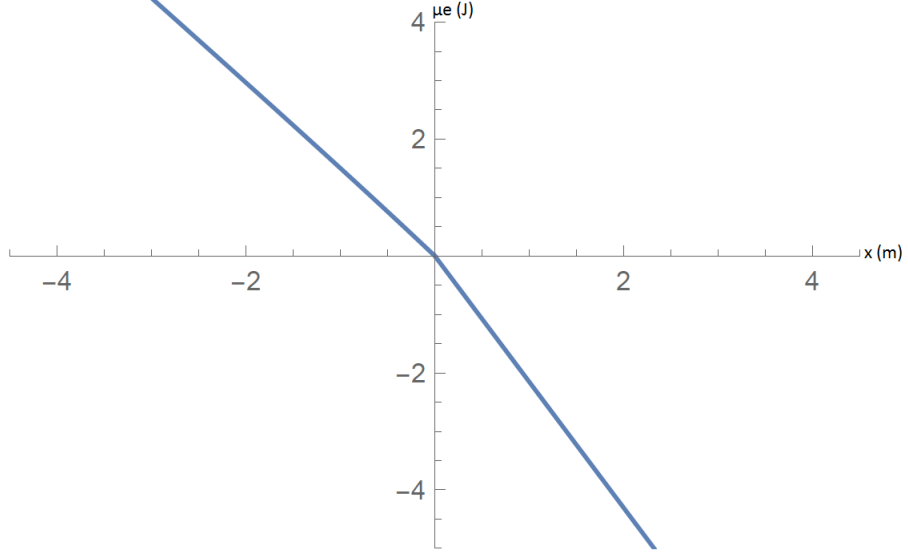
Figure 3: The chemical potential μ_e as a function of x.

For μ_s we expect other behaviour. This is due to the fact that the accumulation of μ_s is not associated with higher energy. μ_s accumulates because $j_+ \neq j_-$ for $x < 0$, but $j_+ = j_-$ for $x > 0$. Since j_e is the same for every x, this implies that there are two possible cases. Namely j_+ has to speed up and j_- has to slow down when passing x=0, or vice versa. When considering a volume element around $x = 0$ you will find a difference from $j_{+/-}$ entering from the left compared to $j_{+/-}$ leaving from the right. Therefore there is accumulation. The accumulation will however not continue forever. One can see in equation 7 that spin relaxation is proportional to μ_s. When μ_s is big enough the spin relaxation will therefore balance the accumulation. Hence there are steady state solutions possible. See for one of those solutions figure 4.
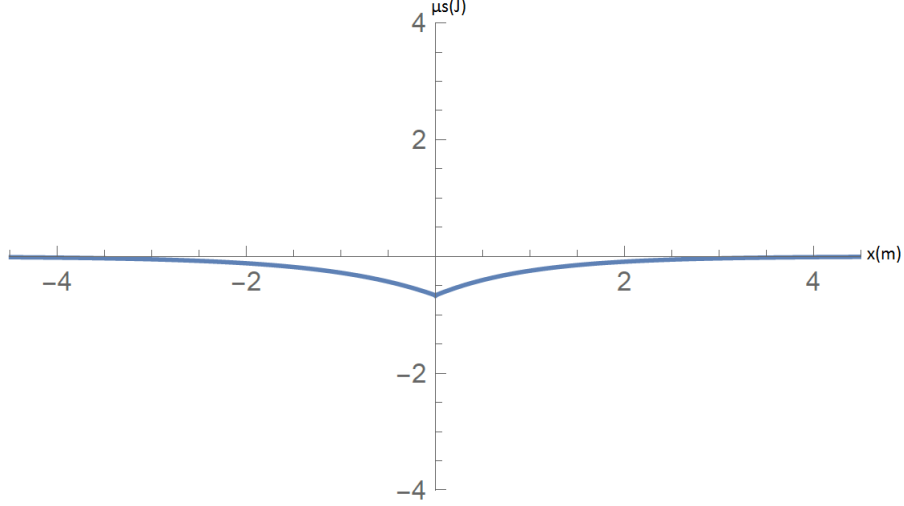
Figure 4: The spin current for $x < 0$ and $x > 0$ differ. Therefore spin currents accumulate around $x = 0$.

3.2 Time dependent solution

To take into account the time dependent behavior, we have to take into account the time derivatives in equation 6 and 7. It is convenient to rewrite the derivative the following way:

$$\frac{\partial \rho}{\partial t} = \frac{\partial \rho}{\partial \mu_\pm} \frac{\partial \mu_\pm}{\partial t} \tag{13}$$

and

$$\rho = \int d\epsilon \, n_F(\epsilon) \nu(\epsilon), \tag{14}$$

with n_F the Fermi-Dirac distribution and $\nu(\epsilon)$ the density of states. Since we stay well below the Fermi temperature in the experiment, we can approximate $n_F(\epsilon) \approx \Theta(\epsilon_F - \epsilon)$ with Θ the Heaviside step-function. Taking the the derivative of ρ with respect to $\mu_\pm$ we obtain

$$\frac{\partial \rho}{\partial \mu_\pm} = \int d\epsilon \frac{\partial n_F(\epsilon)}{\partial \mu_\pm} \nu(\epsilon). \tag{15}$$

Because $\nu(\epsilon)$ is independent of $\mu_\pm$ and $\partial n_F(\epsilon)/\partial \mu_\pm = \delta(\epsilon_F - \epsilon)$, this implies

$$\nu(\mu_\pm) = \frac{\partial \rho}{\partial \mu_\pm}, \tag{16}$$

with ν the density of states. For NM the following relation holds for the density of states: $\nu(\mu_+) = \nu(\mu_-) = \nu(\epsilon_F)$ with ϵ_F the Fermi energy. Combined with (5),(6) and (7) we obtain

$$\nu(\epsilon_F) \frac{\partial \mu_+}{\partial t} - \sigma \nabla^2 \mu_+ = -\frac{\Gamma}{2}(\mu_+ - \mu_-); \tag{17}$$

$$\nu(\epsilon_F) \frac{\partial \mu_-}{\partial t} - \sigma \nabla^2 \mu_- = \frac{\Gamma}{2}(\mu_+ - \mu_-). \tag{18}$$

9

These equations cannot be solved analytically. It is however solvable when the spatial part is discretized. So $\mu_\pm(x,t) \to \mu_{\pm,i}(t)$ and $\nabla^2\mu_\pm(x,t) \to (\mu_{\pm,i+1}(t) + \mu_{\pm,i-1}(t) - 2\mu_{\pm,i}(t))/\epsilon^2$, with ϵ the distance between i and $i+1$ for every i.

For the numerical calculation we also want to make equation (17) and (18) dimensionless. Therefore we re-scale $t \to \tilde{t}$ with a constant in the following fashion:

$$\tilde{t} = \frac{\Gamma}{e\nu(\epsilon_F)}t. \tag{19}$$

This changes (17) and (18) in

$$\frac{\partial\mu_{\pm,i}}{\partial\tilde{t}} = \eta(\mu_{\pm,i+1} + \mu_{\pm,i-1} - 2\mu_{\pm,i}) \mp \frac{1}{2}(\mu_{+,i} - \mu_{-,i}), \tag{20}$$

with $\eta = \sigma/e\Gamma\epsilon^2$.

Now we are going to derive the equations for FM. The total conductivity for NM and FM are not the same in general. Therefore $k\sigma = \sigma_{FM}$, with σ the conductivity of NM, σ_{FM} the conductivity of FM and $k \in [0,\infty]$. For FM the density of states in equilibrium is also in general not equal for spin up and down, so $\nu(\mu_+) \neq \nu(\mu_-)$ and $\sigma_+ \neq \sigma_-$. With the same procedure we obtain the following expressions for FM:

$$\frac{\partial\mu_{+,i}}{\partial\tilde{t}} = \alpha k\frac{\nu(\epsilon_F)}{\nu_F(\mu_+)}\eta(\mu_{+,i+1} + \mu_{+,i-1} - 2\mu_{+,i}) - \frac{\nu(\epsilon_F)}{2\nu_F(\mu_+)}(\mu_{+,i} - \mu_{-,i}); \tag{21}$$

$$\frac{\partial\mu_{-,i}}{\partial\tilde{t}} = (1-\alpha)k\frac{\nu(\epsilon_F)}{\nu_F(\mu_-)}\eta(\mu_{-,i+1} + \mu_{-,i-1} - 2\mu_{-,i}) + \frac{\nu(\epsilon_F)}{2\nu_F(\mu_-)}(\mu_{+,i} - \mu_{-,i}). \tag{22}$$

We solved for $\mu_{-,i}$ and $\mu_{+,i}$ with respect to t for $i = 1$ till $i = 20$ and subsequently plotted $\mu_{s,i}(t)/\mu_{s,i}(0) = (\mu_{+,i} - \mu_{-,i})/\mu_{s,i}(0)$. As a starting condition for $\mu_{s,i}(0)$ we used a step function which is a greater than zero constant for $i < 11$ and 0 for $i > 10$. The results are shown in figure 5.
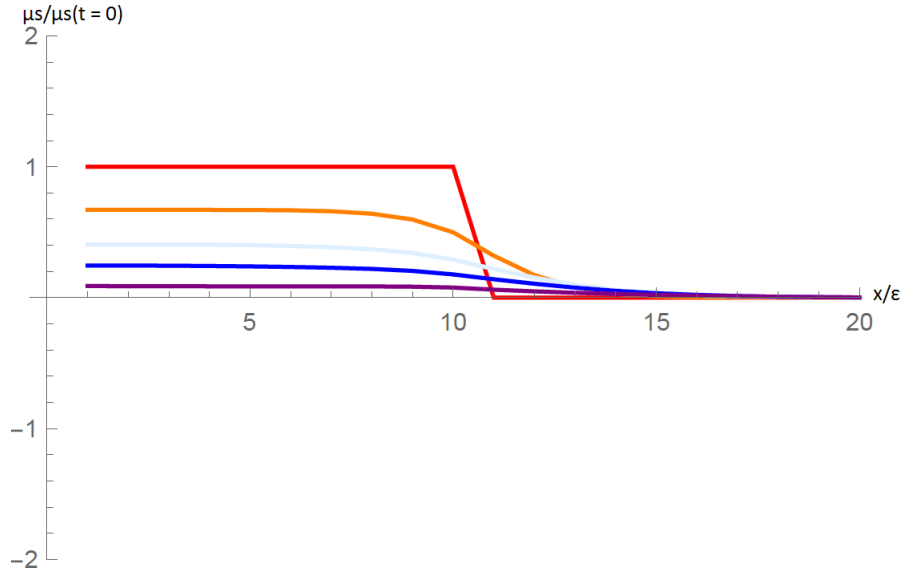

Figure 5: The increase in time is in the order red, orange, light blue, blue, purple. As a function of time one observes μ_s diffusing from high to low values. Beside this effect there is also a relaxation term, which reduces the total μ_s as time passes.

We clearly see both diffusion and spin relaxation playing a part in the time evolution of μ_s. Diffusion is due to the first terms of the RHS of equation 21 and 22. It causes μ_s to spread out to the NM. It however does not cause μ_s to decrease to zero.This behaviour is namely induced by the spin relaxation terms, which is the last term of equation 21 and 22. Without the spin relaxation μ_s would become a non zero constant, which is not observed in the plot.

We elaborate the system to obtain a more general description by choosing different Γ for NM and FM. Hereby we choose $\Gamma \to \Gamma_{NM}$ for NM and $\Gamma \to \Gamma_{FM}$ for FM. Because Γ_{NM} and Γ_{FM} are constants, we can write

$$\Gamma_{FM} = \Gamma_{NM} + \delta\Gamma. \tag{23}$$

For this more general system we redefine $\tilde{t}$ as

$$\tilde{t} = \frac{\Gamma_{NM}}{e\nu(\epsilon_F)}t, \tag{24}$$

and redefine η as

$$\eta = \frac{\sigma}{e\Gamma_{NM}\epsilon}. \tag{25}$$

The discretized equations (20) for NM stay the same. The equations for FM change in:

$$\frac{\partial\mu_{+,i}}{\partial\tilde{t}} = \alpha k\frac{\nu(\epsilon_F)}{\nu_F(\mu_+)}\eta(\mu_{+,i+1} + \mu_{+,i-1} - 2\mu_{+,i}) - \frac{\nu(\epsilon_F)}{2\nu_F(\mu_+)}(1 + \Gamma_R)(\mu_{+,i} - \mu_{-,i}), \tag{26}$$

$$\frac{\partial\mu_{-,i}}{\partial\tilde{t}} = (1 - \alpha)k\frac{\nu(\epsilon_F)}{\nu_F(\mu_-)}\eta(\mu_{-,i+1} + \mu_{-,i-1} - 2\mu_{-,i}) + \frac{\nu(\epsilon_F)}{2\nu_F(\mu_-)}(1 + \Gamma_R)(\mu_{+,i} - \mu_{-,i}), \tag{27}$$

with $\Gamma_R \equiv \delta\Gamma/\Gamma_{NM}$. This enables us to consider a few interesting limits.

When $\Gamma_{FM} \gg \Gamma_{NM}$ and η is normal[2], the FM will demagnetize quickly due to spin relaxation. Yet a small amount of magnetization will flow to the NM, since η is nonzero. Γ_{FM} however is very big, therefore there is such a fast decrease of magnetization in FM that it will go faster to 0 than the bit of magnetization that went to NM. This causes a gradient to go from NM to FM. Therefore at some point in time there is a little bit of magnetization around the interface. See for this phenomenon figure 6

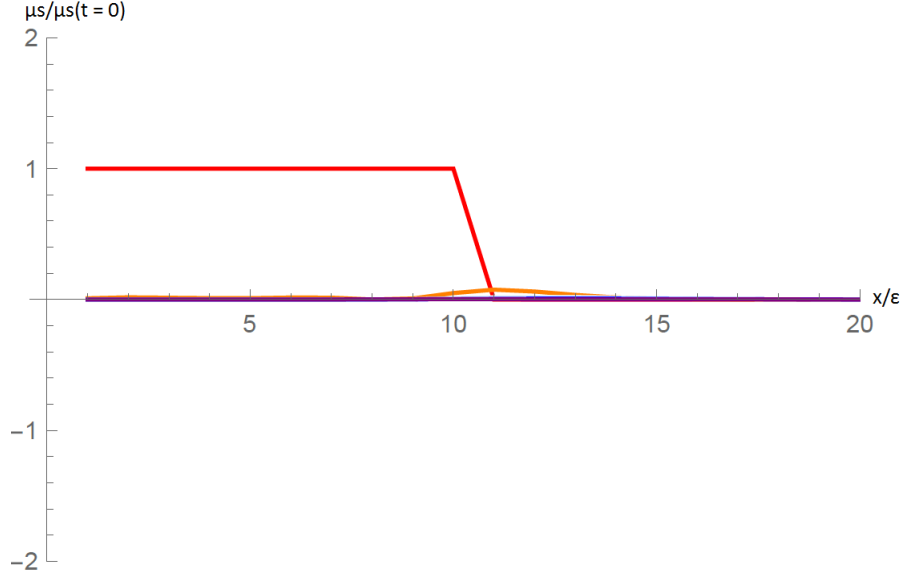[2]When talking about big, small, and normal in this section, we mean compared to figure 5

Figure 6: The increase in time is in the order red, orange, light blue, blue, purple. Very high spin relaxation Γ_{FM}, with $\Gamma_{FM} \gg \Gamma_{NM}$, and diffusion comparable to figure 5.

In figure 7 you can see the limit of $\Gamma_{FM} = 0$ and η is normal. Since we picked η the same as in figure 5 the diffusion is comparable. There is however no spin relaxation in the FM part, only in the NM part. Therefore it takes longer to demagnetize completely. This is precisely what we observe.
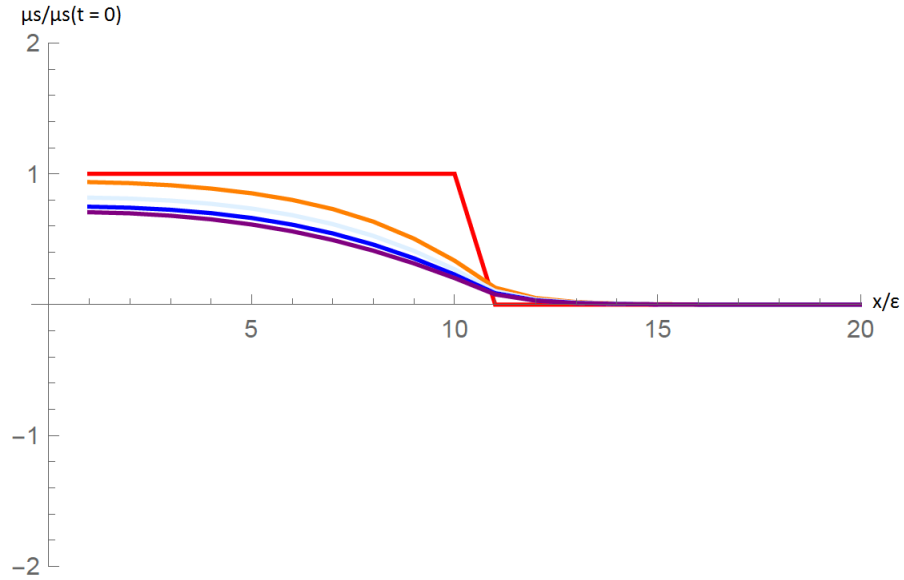

Figure 7: The increase in time is in the order red, orange, light blue, blue, purple. $\Gamma_{FM} = 0$ and normal diffusion.

When η is small and the relaxation times are normal, you would expect the magnetization to decrease as a function of time while the magnetization is barely flowing. This is exactly what we observe in figure 8.
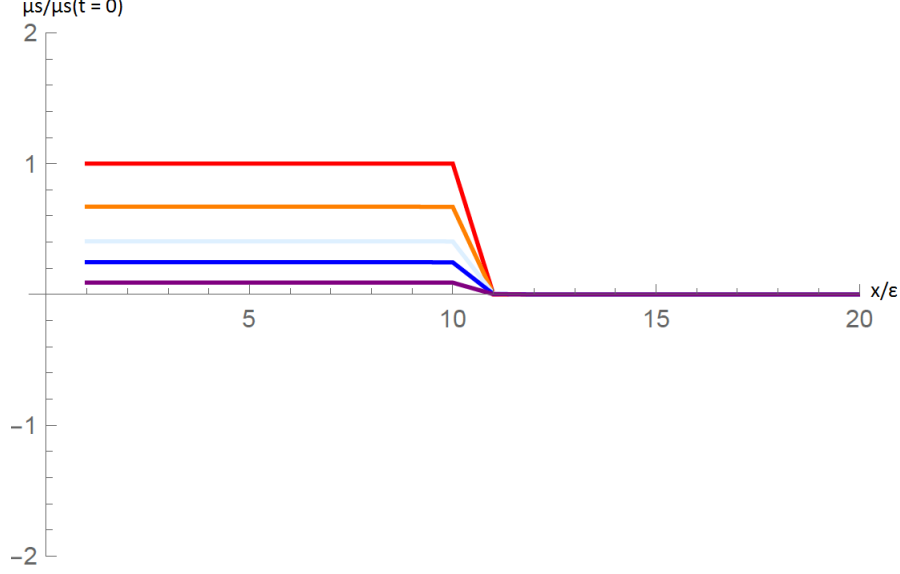
Figure 8: The increase in time is in the order red, orange, light blue, blue, purple. For very small diffusion compared to figure 5 and $\Gamma_{FM} = \Gamma_{NM}$ comparable to it.

4 Combining M3TM with spin transport

For combining M3TM with spin transport, Koopmans proposed the following differential equation[3]:

$$\frac{d\Delta m}{dt} = \frac{V_{at}}{e^2}\nabla\sigma\nabla\left(\frac{\Delta m}{\nu_f}\right) + \frac{dm}{dt}\bigg|_{M3TM} - \frac{dm_{eq}(T_e)}{dt}, \tag{28}$$

with $\Delta m = m - m_{eq}$, V_{at} the volume of a unit cell, $dm/dt|_{M3TM}$ the local change of demagnetization given by expression 3, and $dm_{eq}(T_e)/dt$ the magnetization is equilibrium, thus $dm/dt|_{M3TM} = 0$. To justify this formula, consider

$$\frac{d\Delta m}{dt} = \frac{dm}{dt} - \frac{dm_{eq}}{dt}. \tag{29}$$

The change in magnetization can be caused by local changes in magnetization and transport of magnetization. The former we have already described with the M3TM. The latter is given by non local changes, thus through spin transport. Therefore the following relation holds

$$\frac{dm}{dt} = \frac{dm}{dt}\bigg|_{Spintransport} + \frac{dm}{dt}\bigg|_{M3TM}, \tag{30}$$

where

$$\frac{dm}{dt}\bigg|_{Spintransport} = \frac{V_{at}}{e^2}\nabla\sigma\nabla\left(\frac{\Delta m}{\nu_f}\right). \tag{31}$$

To be able to easily find numerical solutions we linearize the M3TM, thus

$$\frac{dm}{dt}\bigg|_{M3TM} = -\frac{1}{\tau}\Delta m, \tag{32}$$

13

with

$$\tau = \left(Rm_{eq} \frac{T_p}{T_c} \frac{d}{dm} \left(1 - m \coth \left(\frac{mT_c}{T_e} \right) \right) \Big|_{\Delta m = 0} \right)^{-1}. \tag{33}$$

Thus

$$\tau = \left(Rm_{eq} \frac{T_p}{T_c} \left(\frac{m_{eq}T_c}{T_e} \left(\coth^2 \left(\frac{m_{eq}T_c}{T_e} \right) - 1 \right) - \coth \left(\frac{m_{eq}T_c}{T_e} \right) \right) \right)^{-1}. \tag{34}$$

We also write

$$\frac{dm_{eq}}{dt} = \frac{dm_{eq}}{dT_e} \frac{dT_e}{dt}, \tag{35}$$

this implies

$$\frac{d\Delta m}{dt} = \frac{V_{at}}{e^2} \nabla \sigma \nabla \left(\frac{\Delta m}{\nu_f} \right) - \frac{1}{\tau} \Delta m - \frac{dm_{eq}}{dT_e} \frac{dT_e}{dt}. \tag{36}$$

5 Conclusion

In this thesis we reviewed the M3TM and its shortcomings. We found that one important shortcoming is the lack of spin transport. The M3TM is only a local theory. Realizing this we started reviewing spin transport and considered a few examples. We finished with a theory proposed by Koopmans which combines the M3TM with spin transport.[3] For further research it would be interesting to reproduce the experiment of Malinowski in a simulation grounded on the new theory. Moreover, since the experiments are typically far from equilibrium, investigation into effects beyond linear response need to be incorporated.

References

[1] E. Beaurepaire, et al. *Ultrafast Spin Dynamics in Ferromagnetic Nickle* Physical Review Letters, Volume 76, Number 22, 27 May 1996

[2] B. Koopmans, et al. *Explaining the paradoxial diversity of ultrafast laser-induced demagnetization* Nature Materials, 13 December 2009

[3] B. Koopmans, *private communication*

[4] S. Schellekens, *Manipulating Spins* Proefschrift Eindhoven University for Technology, 3 April 2014

[5] G. Malinowski, et al. *Control of speed and efficiency of ultra-fast demagnetization by direct transfer of spin angular momentum* Nature Physics, Vol 4, November 2008

[6] T. Valet, A. Fert, *Theory of perpendicular magnetoresistance in magnetic multilayers* Physical Review B, 1 September 1993-II